

**Investigating the coupling between phytoplankton biomass,
aerosol optical depth and sea-ice cover in the Greenland Sea**

Author

Gabric, Albert J, Qu, Bo, Matrai, Patricia A, Murphy, Carly, Lu, Hailang, Lin, Dao Rong, Qian, Feng, Zhao, Min

Published

2014

Journal Title

Dynamics of Atmospheres and Oceans

DOI

[10.1016/j.dynatmoce.2014.03.001](https://doi.org/10.1016/j.dynatmoce.2014.03.001)

Rights statement

© 2014 Elsevier B.V. This is the author-manuscript version of this paper. Reproduced in accordance with the copyright policy of the publisher. Please refer to the journal's website for access to the definitive, published version.

Downloaded from

<http://hdl.handle.net/10072/61981>

Griffith Research Online

<https://research-repository.griffith.edu.au>

Investigating the coupling between phytoplankton biomass, aerosol optical depth and sea-ice cover in the Greenland Sea

By Albert J. Gabric^{1*}, Bo Qu², Patricia A. Matrai³, Carly Murphy¹, Hailang Lu², Dao Rong Lin², Feng Qian² and Min Zhao²

¹School of Environment, Griffith University, Nathan, Qld, Australia, 4111; ²School of Science, Nantong University, China, 226007 ; ³Bigelow Laboratory for Ocean Sciences, East Boothbay Harbor, ME 04544, USA

*Corresponding author.

email: a.gabric@griffith.edu.au

ABSTRACT

We investigate the relationship between satellite-derived time series for microalgal biomass, measured using remotely sensed chlorophyll-*a* (CHL: mgm^{-3}), aerosol optical depth (AOD) and sea ice cover (ICE) in the Greenland Sea (10°W - 10°E , 65 - 80°N) over the decadal period 2003-2012. Zonal averages for all variables were computed in 5-degree latitude bands. Unlike other regions of the Arctic Ocean, the marginal ice zone in the Greenland Sea is confined to north of 75°N . The CHL time series is characterised by high interannual variability, especially in the northern marginal sea ice zone (MIZ) where variability in sea ice extent is a likely factor. The ten-year climatology shows that CHL increases from March, reaching a seasonal peak in May in the southern sector and in June in the northern sectors. The climatological peak of AOD is achieved in April in all latitude bands, about a month before the peak in CHL. This suggests that the Arctic aerosol burden is strongly affected by continental sources in early spring.

Interestingly, a summer increase in AOD (which succeeds the CHL maximum) is seen in some years. Sea ice extent in early spring is less than 40% in the northern sector in all years. There is considerable interannual variability in both the onset of melt and the extent of sea ice loss during summer, with the minimum summer sea ice extent decreasing to almost zero in five of the years. Cross-correlation analyses of the three times series identifies a statistically significant relation between CHL and AOD in six of the years in the southern sector, but no correlation between CHL and ICE was found in the northern sector. There is, however, a significant correlation between AOD and ICE time series in the northern sector

in four years. High AOD values registered in early spring are most likely of anthropogenic origin, however, peaks later in summer coincident with the phytoplankton bloom and high emissions of biogenic aerosol precursors such as dimethylsulfide and other primary aerosols of marine origin, suggest the summer atmospheric aerosol burden is likely influenced by biogenic emissions .

Key-words: Arctic, phytoplankton, aerosols, Greenland Sea, sea-ice

1. Introduction

Warming in the Arctic is occurring at a greater rate than other places in the Northern Hemisphere, and this trend is expected to continue into the future. During the past century, glaciers have receded throughout the Arctic, terrestrial ecosystems have advanced northward, and perennial Arctic Ocean (AO) sea ice has diminished (Miller et al., 2003; Wang and Overland, 2009). Taken together, the size and speed of the summer sea-ice loss over the last few decades is highly unusual compared to events from previous thousands of years (Kwok and Rothrock, 2009). The impacts of a general loss of perennial sea ice are likely to be far-reaching, and include both feedbacks on the regional heat budget (the “sea-ice albedo effect”) and perturbations to the Arctic marine food web (Gabric et al., 2005a; Holland et al., 2006; Post et al., 2013), however, our current knowledge of changes in regional planktonic and benthic systems is surprisingly low (Wassmann et al., 2011).

A critical component of the Arctic marine food web are sea-ice algae which begin to grow in early spring within and underneath the ice, producing a substantial biomass despite very low light intensities (Gradinger, 2009). Pelagic algal blooms, in contrast, normally occur after ice breakup, at high latitudes as late as July-September. Changes in the timing of ice melt and breakup can cause a mismatch between primary and secondary producers, with negative consequences for the entire Arctic marine food web. Zhang et al. (2010) simulate a generally downward trend in summer sea-ice extent during 1988-2007 and a steady decrease in Arctic sea-ice thickness, leading to an increase in simulated photosynthetically active radiation (PAR) at the ocean surface (+43%) and primary production (PP) (+50%) in

sea ice covered areas over the 19-year period. In contrast to other parts of the Arctic, the Greenland Sea shows a statistically significant decreasing trend in satellite-derived annual NPP and bloom duration for the 1998-2009 period, which is yet to be explained (Arrigo and van Dijken, 2011). Additionally, Kahru et al. (2011) analysed a time series of satellite-derived chlorophyll-a for the period 1997-2009 to examine the phenology of the annual phytoplankton bloom and detected statistically significant trends towards earlier phytoplankton blooms in about 11% of the AO area.

Aerosol concentration in the Arctic atmosphere varies seasonally, with continental anthropogenic sources dominant during winter and early spring (Heidam, 1984; Quinn et al., 2007) and local marine biogenic sources contributing to the aerosol burden during summer and autumn (Chang et al., 2011b; Rempillo et al., 2011; Park et al., 2013). A connection between spring-summer sea-ice melt and increased emission of radiatively active biogenic aerosols, such as dimethylsulfide (DMS), has been observed in Antarctic waters (Trevena and Jones, 2012) and predicted for the AO (Gabric et al., 2005a). The nexus between seasonal sea-ice loss in the Arctic and DMS cycling is the subject of a recent review by Levasseur (2013).

Field studies in the Arctic have noted complex inter-relationships between phytoplankton growth, sea-ice melt and the formation and emission of biogenic aerosol precursors such as DMS (Leck et al., 1996; Matrai et al., 2008; Luce et al., 2011). Our aim here is to understand what drives the connection between sea-ice and key ecological metrics, such as phytoplankton standing stock and biogenic aerosol production. There is little research

utilising the existing remote sensing data archive to examine the relationship between biological parameters, sea-ice extent and aerosol parameters in the AO. We attempt to fill this knowledge gap by examining the temporal and spatial coherence between satellite-derived estimates of surface chlorophyll *a* (CHL) (a proxy for algal biomass), sea-ice extent (ICE), and aerosol optical depth (AOD) which is related to the atmospheric burden of aerosols.

2. Characteristics of the study region

The study region (10°W-10°E, 65°-80°N) covers a large part of the Greenland Sea (Figure 1), which lies south of the Arctic Basin proper and borders Greenland (west), Svalbard (east), the main AO basin (north), and the Norwegian Sea and Iceland (south) (Figure 1). This region has southern and northern boundary lengths of 935km and 384km, respectively, and a north-south dimension of 1668km. Average depth is 1450 m, with the deepest recorded point at 4800 m, where it merges with the Barents and Norwegian Seas. The bathymetry of the region controls the exchange of water masses between the Arctic basin and the North Atlantic Ocean. The Greenland Sea is thought to be especially important in terms of the transfer of atmospheric carbon to the deep ocean as it is an area of surface convergence and North Atlantic deep-water formation (Rudels et al., 1991; Schmitz, 1995).

2.1 Major Currents

The Fram Strait (Figure 1), between Greenland and Svalbard, is very important with regard to heat and mass exchange in the AO, representing the only deep water connection between

the AO and the rest of the world ocean. Arctic freshwater, stored in the upper few hundred meters, is delivered to the North Atlantic through Fram Strait or the Canadian Arctic Archipelago (Beszczynska-Moller et al., 2011). Large quantities of heat carried north by the West Spitsbergen Current (WSC) influence the climate in the Arctic region as a whole (Hop et al., 2006). The East Greenland Current (EGC) carries cold, low salinity Arctic flows southward and turns westward around Cape Farewell, then northward towards the western Greenland coast (Foldvik et al., 1988). The southern current carries warm, saline Atlantic water origin through Davis Strait to the North Water polynya in Smith Sound and then turns west and south again with the Baffin and Labrador currents (Bacle et al., 2002). The transit time is sufficiently long to allow thermohaline and biogeochemical changes during passage (Bacle et al., 2002). The transports of heat, salt and nutrients, as well as plankton, fish eggs and larvae, to Greenland waters by the North Atlantic current systems, are major governing processes affecting the Greenland Sea ecosystem (Hunt and Drinkwater, 2007). Interannual changes in the marine environment and ocean circulation in the Greenland Sea are closely related to fluctuations in the North Atlantic Oscillation (NAO) (Chhak and Moore, 2007), with periods of strong, positive NAO resulting in increases of Atlantic water inflow (Dickson et al., 2000). Hop et al. (2006) found that the minimum or maximum NAO winter index generally corresponds to a minimum or maximum temperature in Fram Strait.

2.2 *Sea-Ice*

A large volume of water and sea ice is transported through Fram Strait, with a net water transport of 2 ± 2.7 Sv southward in the EGC and a volume ice flux in the range of

0.06-0.11 Sv (Kwok et al., 2004). Serreze et al. (2006) estimate that roughly equal contributions from Fram Strait sea-ice and liquid freshwater fluxes deliver about 50% of the freshwater exported from the AO. Sea-ice concentration on the east side of Fram Strait is lower than in the western side and, during summer months, the east side of the strait is almost ice free (Hop et al., 2006). Sea-ice extent reaches a maximum in April, and a minimum by August, with maximum ice-flux export from October through December and a minimum from January to March (Woodgate et al., 1999).

In recent decades, a decline in AO sea-ice coverage, thickness, and volume has been observed, with the largest sea ice retreat in 2012 (Arctic Sea-ice News & Analysis 14 September 2012; <http://nsidc.org/arcticseaicenews/>). Arctic sea ice extent at the end of the melt season in September has declined at a rate of 7.8% per decade from 1953 or as much as 10.3% per decade since 1979, with a higher rate of ice thickness decline compared to the sea-ice extent reduction (Stroeve et al., 2007). An overall rise in surface air temperature over the AO is consistent with the sea ice loss (Comiso, 2003). These changes are likely to have severe ecological consequences for AO biota (Wassmann, 2011; Wassmann and Reigstad, 2011).

2.3 *Phytoplankton*

Primary production in the Arctic is highly seasonal and driven by changes in light conditions, sea-ice cover and nutrient availability (Harrison and Cota, 1991). Pelagic phytoplankton are the major producers of organic matter in open waters, but sea-ice algae begin to grow in early spring within and underneath the ice, producing a substantial

localized biomass despite very low light intensities (Leu et al., 2011). Major primary producers in the sea ice are pennate diatoms and flagellated protists (Ikavalko and Gradinger, 1997). Ice algae contribute up to 25% to local primary production in the Arctic, though it is considered negligible for annual pan-Arctic production (Wassmann et al., 2006), compared with around 5% in the Antarctic (Lizotte, 2001). The projected thinning of sea ice can increase the intensity of under-ice PAR, which is a critical limiting factor for growth of ice algae in early spring, thus enhancing ice-algal production and accelerating phytoplankton production (Zhang et al., 2010; Lee et al., 2011). Pelagic algal blooms, in contrast, normally occur after ice breakup, as late as July-September at high latitudes; however, a few reports of large sub-ice algal blooms have recently been made (Arrigo et al., 2012), perhaps due to enhanced radiation through thinner and pondier sea ice (Lee et al., 2011). Indeed, Heide-Jorgensen et al. (2007) examined the coupling between CHL, sea ice and sea surface temperature (SST) in Disko Bay, West Greenland, and found the abundance of chlorophyll-*a* in low sea ice years was considerably larger than in high sea ice years, due to the effect of more open water on light-induced stimulation of primary production.

Light is the major limiting factor for primary production in Arctic waters with multi-year ice cover, so that the phytoplankton growth season there is restricted to the ice melt period in summer (Spies et al., 1988). North of 65°N, the low nitrate waters of the EGC also control net community production; as these waters travel south, ice-melt and fresh water additions from melting glaciers keep nitrate concentrations low. Phytoplankton blooms in the Greenland Sea start in early May and peak by early June, frequently depleting most of

the available nitrate and phosphate by summer (Cota et al., 1994; Rey et al., 2000). The spring community is mainly composed of diatoms and the prymnesiophyte *Phaeocystis*, which may form intense blooms during April and early May (Smith et al., 1991). Strong stratification occurs in summer due to melt water and solar heating. In summer and autumn, diatoms, such as *Chaetoceros* spp. in surface waters and *Nitzschia* spp. and *Thalassiosira* spp. in deep waters, may dominate the microflora of the Greenland Sea (Spies, 1987). By late October, the rapidly decreasing day length terminates the phytoplankton growth season (Hop et al., 2006).

2.4 *Biogenic Aerosols*

Measurements by Chang et al. (2011a) of sub-micron aerosol in the central AO during summer showed that marine biogenic and continental sources of particles constituted 33% and 36% of the sampled ambient aerosol mass, respectively. Both fractions were predominantly composed of sulfate, with 47% of the sulfate apportioned to marine biogenic sources and 48% to continental sources, by mass. The remaining ambient aerosol mass was apportioned to an organic-rich factor, whose source was unknown, but that could have originated in part from marine microalgae over the high Arctic pack ice and marginal ice zone (MIZ). Large increases in concentration of particles smaller than 20 nm diameter have been observed over the central AO in summer and are often composed of exopolymer secretions of microalgae and bacteria (Leck and Bigg, 2005; Orellana et al., 2011). Thus, a marine biogenic source of aerosols is significant in the high AO in summer, especially for nascent particle populations (Leck and Bigg, 2005; Leck and Bigg, 2010; Russell et al., 2010).

Modelling studies simulate a significant increase in biogenic aerosol production is likely under warming (Gabric et al., 2005a; Ito and Kawamiya, 2010). Analysis of aerosol time series at Alert (Canada, 82.5°N) suggests that the biogenic component of sulfur in those particles increased by 14%, relative to the anthropogenic contribution, between 1993 and 2003 (Norman et al., 2005).

Although limited in number, aerosol field studies during summer in the AO that overlap our study region suggest the time for gas-to-particle transformation and deposition of gas (DMS) or oxidation products (SO₂) on pre-existing particles is very short (~ 1 day) (Kerminen and Leck, 2001; Heintzenberg and Leck, 2012). Similarly fast DMS oxidation rates (~1 d) have also been observed in other ocean regions (Osthoff et al., 2009). Modelling studies of DMS-to-particle transformation in the Canadian Arctic during summer also suggest fast rates (Chang et al., 2011b). Mean summertime wind speeds for our region are typically around 5 ms⁻¹ (Qu et al., 2012), which suggests aerosol precursor compounds emitted from the ocean surface in the centre of our region would have a residence time in the region of at least one day for east-west trajectories and longer for north-south trajectories.

An updated global monthly climatology of surface ocean DMS concentration and sea-to-air emission flux has recently been produced by Lana et al. (2011) who applied interpolation/extrapolation techniques to project the discrete DMS concentration data onto a grid based on biogeographic provinces (Longhurst, 2007). The biogeographic province that overlaps our study region is the Atlantic Arctic, where the cycle in DMS seawater

concentration is strongly seasonal, increasing in April, with peaks in June and August, and then decreasing rapidly in September (Lana et al., 2011).

Aerosol optical depth (AOD) is a quantitative measure of the extinction of solar radiation by aerosol scattering and absorption between the point of observation and the top of the atmosphere and can be used as a proxy for aerosol atmospheric burden. AOD is proportional to aerosol particle concentration from the sea surface to the top of atmosphere (Wang et al., 2000) and is mainly influenced by aerosols in the marine boundary layer and scattering by particles in the size fraction below 10 μm in diameter (Collins et al., 2000). MODIS-retrieved aerosol optical depth falls within the expected uncertainty, differing by only 2% from the AERONET ground-based observations (Remer et al., 2002). Satellite-retrieved AOD will be determined by the atmospheric concentration of a number of chemical species (Remer et al., 2008), including sea-salt, mineral dust, organic compounds, as well as non-sea-salt sulfate and methanesulfonic acid (MSA), the latter being solely derived from the oxidation of gaseous DMS (Gabric et al., 2005b). As noted above, aerosol precursors emitted in our Greenland Sea region will have a residence time of at least one day, which will be long enough for gas-to-particle conversion, and thus possibly affecting summer retrievals of regional mean AOD.

Indeed, a strong relationship between satellite retrieved CHL and AOD during the austral summer in the Subantarctic Southern Ocean has been attributed to emissions of biogenic sulfate aerosols (Gabric et al., 2002). More recently, Gabric et al. (2005b) found that the coherence between remotely sensed (CHL) and AOD time series is strong in the 50-60°S

band, where a time lag between the seasonal peaks was thought to be due to the emission of biogenic aerosol precursors, such as DMS from melting sea ice. This hypothesis was later supported by field measurements of high DMS emissions over sea ice in the Southern Ocean (SO) by Zemmelen et al. (2008).

3. Data and methods

Satellite data on CHL concentration and AOD were obtained from the MODIS (Moderate-resolution Imaging Spectroradiometer)/Aqua, archive (Version 5.1 reprocessing) for the 10-year period 2003-2012, ignoring the incomplete 2002 dataset, as MODIS-Aqua data was first available from July 2002 (King et al., 2003). Compared with ground-based AERONET observations of AOD, MODIS aerosol products estimate AOD to within expected accuracy more than 60% of the time over ocean (Remer et al., 2008). Here we utilise Level-3 (4-km equi-rectangular projection) 8-day mapped data CHL and Level 2 AOD at 550nm and 10km spatial resolution (<http://oceandata.sci.gsfc.nasa.gov/MODISA/Binned/8Day/2009>). The SeaWiFS Data Analysis System (SeaDAS 6.1) was then used for data processing.

Sea ice cover was obtained from the NOAA (NCEP/EMC/CMB) global database at weekly interval and 1x1° spatial resolution from the IRI Data library (http://iridl.ldeo.columbia.edu/expert/SOURCES/.NOAA%20/.NCEP/.EMC/.CMB/.GLOBAL/.Reyn_SmithOiv2/.weekly/sea_ice/). Due to high sea-ice coverage and high zenith angle of the sun in the Arctic, CHL and AOD data are only available from 85°N southwards

and for certain times of the year (Mar-Sept). Due to the possible contamination of pixels by sea ice north of 80°N (Belanger et al., 2007), our study area was restricted to the Greenland Sea from 65-80°N.

Both monthly mean and eight-day mean CHL and AOD and weekly ICE were retrieved in the entire study region over the study time period. Due to meridional variability in sea ice cover and light regimes, we divided the study region into three 5-degree latitude sectors, and computed zonal averages for the parameters of interest in each sector.

Time series of biophysical data are often auto-correlated, as natural systems tend to vary smoothly, with sharp discontinuities rarely observed (Jassby and Powell, 1990). Prior to conducting the correlation analyses, mean square successive difference tests were applied to the time series to gauge the extent of serial correlation in the time series for CHL, AOD and ICE (Zar, 1999). After removing auto-correlation by sequential differencing (Chatfield, 2004), cross-correlation coefficients are computed between pairs of the residual time series: CHL-AOD, CHL- ICE, and AOD- ICE. The weekly sea-ice data was interpolated to octads for the correlation analyses with the CHL and AOD time series. Field data on DMS sea-water concentrations for the study region sampled at irregular intervals for the period 1990-2008 were obtained from the NOAA-maintained database (<http://saga.pmel.noaa.gov/dms/select.php>).

3. Results and discussion

Cloud cover is high in the Arctic and consequently satellite retrievals in the study region

were usually limited to between 10-15% of the total available pixels. This leads to the possibility of bias in estimation of the spatially averaged CHL and AOD values.

3.1 The spatio-temporal distribution of CHL

The 10-year monthly mean CHL climatology (for months of the year when data were available) is shown in Figure 2 and the 8-day data is summarized in Table 1. As expected for polar regions, seasonality in biomass is marked with CHL increasing rapidly from March, reaching a peak (monthly mean $\sim 1.1 \text{ mg m}^{-3}$) during May in ice-free waters (65-70°N) or during June at the higher latitudes. Higher seasonal peak CHL values (mean $\sim 1.3 \text{ mg m}^{-3}$) were achieved at the higher latitudes, but variance about the mean was also quite high (Figure 2b), reflecting interannual variability over our study time period. It is interesting to note the higher CHL variability in the two northern sectors (Figure 2b), which is likely due to interannual variability in the extent and timing of sea ice retreat in the MIZ (Pabi et al., 2008). The 8-day data (Table 1) confirm the general patterns found from the monthly climatology, but reveal slightly higher CHL peak values are achieved in some years.

The Hovmoller plot for CHL (Figure 3a) clearly illustrates the decoupling in the phenology of the bloom between ice-free southern sectors and northern marginal sea ice zones. The seasonal peak in the zonal average CHL occurs in June at 72-75°N, which coincides approximately with the southern limit of the marginal ice zone (MIZ), the boundary between the open ocean and ice-covered seas (fast ice) in the Greenland Sea. As the ice edge retreats north during the summer, CHL increases at the higher latitudes (Figure 3c).

Although corroborating field studies in the Greenland Sea are very limited in both space and time, data collected in a series of cruises during the 1990s, showed a pattern of repeated blooms during the summer season at the ice edge (Richardson et al., 2005) which is consistent with the climatological picture described here.

In the 65-70°N sector, which experiences a longer growing season, there is a distinct increase in CHL during September in several years, e.g. 2008, 2009, 2011, the extent of which cannot be fully captured in the satellite record due to the polar sunset in October (Figure 4a). This is broadly consistent with the field data, which records blooms in both June and August (Richardson et al., 2005).

3.2 The spatio-temporal distribution of AOD

Over the study region, there was a moderate seasonality in AOD, with monthly mean AOD generally higher during spring, and lower in summer (Figure 5a). The peak in AOD occurs during April, before the annual peak in CHL, and is likely due to advection of continental anthropogenic sources (Quinn et al., 2007). Compared with CHL, the relative variance in AOD is lower (Figure 5b), and peaks during June in the two southern sectors, which suggests the influence of biogenic aerosols. The Hovmoller plot for AOD (Figure 3b) shows the seasonal and latitudinal variation in monthly mean AOD and suggests a meridional gradient with higher values sustained in the southern sectors throughout the summer.

Correlation between CHL and AOD time series is statistically significant in six out of ten

years in the southern ice-free sectors (Figure 4 and Table 2), suggesting a coupling between ocean biological processes and atmospheric chemistry. In summer, anthropogenic sources are reduced (Heintzenberg and Leck, 1994), and the aerosol burden will be influenced by the formation of biogenic aerosols, such as DMS and its oxidation product MSA during and following a phytoplankton bloom. Measurements made by Heintzenberg & Leck (1994) at Spitsbergen (12°E, 79°N), just to the east of our study region, record a clear MSA peak in June and July, with the influence of Arctic haze dominant from November to April. Our monthly AOD climatology (Figure 5a) records high variability during June in 65-75°N (Figure 5b), which is consistent with high MSA concentrations having an influence on AOD at this time of the year. Additionally, the monthly AOD time series for 65-70°N shows the presence of a distinct secondary peak from June to August in some years (Figure 5c). In some years (e.g. 2005, 2008) the correlation between CHL and AOD is strong (Table 2), and the AOD time series displays elevated values in summer. This is particularly evident in the ice-free sector (65-70°N) where the AOD time series displays a peak pre-bloom (presumably unrelated to biological emissions) and a clear increase in the post-bloom period during summer (Figure 6a,b).

Further evidence for a mid-summer increase in biogenic aerosol emissions come from modelling studies which show Arctic DMS seawater concentration and sea-to-air flux are elevated for up to three months following the spring bloom (Gabric et al., 2005a). These aerosol precursors can be emitted from open water or from leads in melting sea ice, as has been observed in Antarctic waters (Zemmelink et al., 2008) and Arctic waters (Chen et al., 2012; Sharma et al., 2012) or from injection of nascent primary organic aerosols (Leck et al.

2005). This is further supported by DMS seawater observations in our study region (Figure 7) and the Lana et al. (2011) climatology for the larger Atlantic Arctic province (that encompasses our study region), which show that DMS seawater concentration is elevated from May to August.

3.3 *The impacts of sea ice*

Annual mean sea-ice cover shows a strong meridional gradient in all years, with little ice present south of 75°N (Figure 3c) and zonal mean extent <40% (Figure 4c). This is consistent with other pan-Arctic studies that note the two Atlantic-influenced regions (Greenland Sea and the adjacent Barents Sea) contain a high proportion of open water year-round, while other parts of the AO are much more heavily dominated by sea ice (Arrigo and van Dijken, 2011).

Zonal mean sea ice extent in 75-80°N at the start of spring varied between 30-40%. There is considerable interannual variability in both the timing of melt and the extent of sea ice loss during summer, with the onset of ice melt occurring as early as March in 2004 and as late as June in 2003. In years 2003, 2004, 2006, 2008 and 2010 the northern sector was almost completely ice-free by late August or early September (Figure 4c).

There is no clear relationship between the timing of the onset of ice melt and biomass increase in the 75-80°N sector, and there is no significant correlation between CHL and ICE in any year (Table 2). For example, in 2008, 2010 and 2011, when CHL reached unusually high values – more than double the June climatological mean - , the peak in CHL

occurs while ice extent is still over 25% (Figure 4c). However, in years 2003 and 2004, which were characterised by late and early onset of sea ice melt, respectively, there is little difference in the maximum CHL value achieved.

Interestingly, there is a statistically significant correlation between AOD and ICE in 75-80°N in four of the years: 2006, 2007, 2009, 2011 (Table 2), and it should be noted that each of these years was characterised by late onset of sea ice melt (Figure 4c). Recently, a revised view of the role of sea ice in mediating sea-air gas fluxes has been proposed (Loose et al., 2011). It is being increasingly recognized that the porous nature of sea ice not only provides a habitat for ice algae, but also opens a pathway for exchanges of organic matter, nutrients, gases with seawater below and the atmosphere above. A satellite-based study in the SO found a correlation between CHL, the production of biogenic aerosols and AOD (Gabric et al., 2005b). Field studies in the SO confirm the role of sea ice as a significant source of aerosol precursors, with very high concentrations of DMS and related compounds measured in Antarctic sea ice (Asher et al., 2011) and DMS sea-to-air fluxes from the MIZ also high during the melt period (Zemmelink et al., 2008; Trevena and Jones, 2012).

4. Conclusions

We have examined 10-year, satellite-derived time series of phytoplankton biomass, aerosol optical depth and sea-ice extent in five-degree latitude sectors in the Greenland Sea, which span open water and marginal sea ice zones. The CHL time series is characterised by high interannual variability, especially in the northern MIZ where variability in sea ice extent is

a likely factor. The climatological mean CHL cycle shows that biomass peaks in May in the southern sector (65-70°N), and is followed by a separate bloom in the northern MIZ during June, with high values ($>0.8 \text{ mg m}^{-3}$) through July. CHL in the southern sector is sustained at high values ($> 0.6 \text{ mg m}^{-3}$) through September.

AOD across the study region peaks in April, before the spring phytoplankton bloom, and is likely due to polluted continental air masses advected from the south. AOD in the southern sector remains above 0.06 throughout summer, even though continental sources are reduced at this time of year. The AOD monthly climatology displays a high variance during June, and a secondary summer peak in AOD in 65-70°N is clearly evident in four of the years. This is consistent with the field measurements of aerosol precursors from biogenic sources that lead to sulphate and MSA, and which are elevated in June-August. It is notable that in six of the years, AOD and CHL time series display a statistically significant correlation in the ice-free southern sector (65-70°N), suggesting a possible influence of biogenic emissions on AOD.

Sea ice in the study region is largely confined to north of 75°N, with maximum extent at the start of spring usually less than 40%. The seasonal onset of sea ice melt was highly variable during the time period, starting as early as March or as late as June and as a consequence, there is no clear relationship between CHL and sea ice cover. Summer minimum ice cover north of 75°N is close to zero ($< 5\%$) in five of the years. Our results show that AOD and ICE are correlated in some years, in the northern sector. A nexus between sea ice extent, phytoplankton growth and emission of biogenic aerosols has been found in the SO, which

suggests that the negative trend in Arctic sea ice cover may have an impact on future regional emissions of biogenic aerosols, especially during mid to late summer.

5. Acknowledgements

We thank the NASA Ocean Biology Processing Group for MODIS chlorophyll-*a* (CHL), and aerosol optical depth (AOD) eight-day mapped Aqua data (<http://modis.gsfc.nasa.gov>), and the SeaDAS Development Group for providing the visualization package used (<http://oceancolor.gsfc.nasa.gov/seadas/>). We thank the providers of monthly and weekly Sea Ice Concentration product (NOAA NCEP EMC CMB GLOBAL Reyn_SmithOIv2) and the DMS seawater data, which were obtained from the NOAA Pacific Marine Environmental Laboratory (<http://saga.pmel.noaa.gov/dms>). Finally, we gratefully acknowledge the financial assistance by Nantong University, Jiangsu, China (Research Funding: 09R02) and Chinese National Natural Science Funding (No. 41276097).

REFERENCES

- Arrigo, K. R. and van Dijken, G. L. 2011. Secular trends in Arctic Ocean net primary production. *J. Geophys. Res.-Oceans* **116**.
- Arrigo, K. R., Perovich, D. K., Pickart, R. S., Brown, Z. W., van Dijken, G. L. and co-authors 2012. Massive Phytoplankton Blooms Under Arctic Sea Ice. *Science* **336**, 1408-1408.
- Asher, E. C., Dacey, J. W. H., Mills, M. M., Arrigo, K. R. and Tortell, P. D. 2011. High concentrations and turnover rates of DMS, DMSP and DMSO in Antarctic sea ice. *Geophys. Res. Lett.* **38**.
- Bacle, J., Carmack, E. C. and Ingram, R. G. 2002. Water column structure and circulation under the North Water during spring transition: April-July 1998. *Deep-Sea Research Part II-Topical Studies in Oceanography* **49**, 4907-4925.
- Belanger, S., Ehn, J. K. and Babin, M. 2007. Impact of sea ice on the retrieval of water-leaving reflectance, chlorophyll a concentration and inherent optical properties from satellite ocean color data. *Remote Sensing of Environment* **111**, 51-68.
- Beszczyńska-Moller, A., Woodgate, R. A., Lee, C., Melling, H. and Karcher, M. 2011. A Synthesis of Exchanges Through the Main Oceanic Gateways to the Arctic Ocean. *Oceanography* **24**, 82-99.
- Chang, R. Y. W., Leck, C., Graus, M., Mueller, M., Paatero, J. and co-authors 2011a. Aerosol composition and sources in the central Arctic Ocean during ASCOS. *Atmospheric Chemistry and Physics* **11**, 10619-10636.
- Chang, R. Y. W., Sjostedt, S. J., Pierce, J. R., Papakyriakou, T. N., Scarratt, M. G. and co-authors 2011b. Relating atmospheric and oceanic DMS levels to particle nucleation events in the Canadian Arctic. *Journal of Geophysical Research-Atmospheres* **116**.
- Chatfield, C. 2004. *The Analysis of Time Series: An Introduction, Sixth Edition*. Boca Raton, Florida, CRC Press LLC.
- Chen, L. Q., Wang, J. J., Gao, Y., Xu, G. J., Yang, X. L. and co-authors 2012. Latitudinal distributions of atmospheric MSA and MSA/nss-SO₄²⁻ ratios in summer over the high latitude regions of the Southern and Northern Hemispheres. *J. Geophys. Res.-Atmos.* **117**.
- Chhak, K. C. and Moore, A. M. 2007. The North Atlantic Oscillation as a source of stochastic forcing of the wind-driven ocean circulation. *Dynamics of Atmospheres and Oceans* **43**, 151-170.
- Collins, D. R., Jonsson, H. H., Seinfeld, J. H., Flagan, R. C., Gasso, S. and co-authors 2000. In situ aerosol-size distributions and clear-column radiative closure during ACE-2. *Tellus Ser. B-Chem. Phys. Meteorol.* **52**, 498-525.
- Comiso, J. C. 2003. Warming trends in the Arctic from clear sky satellite observations. *J. Clim.* **16**, 3498-3510.
- Cota, G. F., Smith, W. O. and Mitchell, B. G. 1994. Photosynthesis of Phaeocystis in the Greenland Sea *Limnol. Oceanogr.* **39**, 948-953.

- Dickson, R. R., Osborn, T. J., Hurrell, J. W., Meincke, J., Blindheim, J. and co-authors 2000. The Arctic Ocean response to the North Atlantic oscillation. *J. Clim.* **13**, 2671-2696.
- Foldvik, A., Aagaard, K. and Torresen, T. 1988. On the velocity field of the East Greenland Current. *Deep-Sea Research Part a-Oceanographic Research Papers* **35**, 1335-1354.
- Gabric, A. J., Cropp, R., Ayers, G. P., McTainsh, G. and Braddock, R. 2002. Coupling between cycles of phytoplankton biomass and aerosol optical depth as derived from SeaWiFS time series in the Subantarctic Southern Ocean - art. no. 1112. *Geophys. Res. Lett.* **29**, 1112-1112.
- Gabric, A. J., Qu, B., Matrai, P. A. and Hirst, A. C. 2005a. The simulated response of dimethylsulfide production in the Arctic Ocean to global warming. *Tellus B* **57**, 391-403.
- Gabric, A. J., Shephard, J. M., Knight, J. M., Jones, G. and Trevena, A. J. 2005b. Correlations between the satellite-derived seasonal cycles of phytoplankton biomass and aerosol optical depth in the Southern Ocean: Evidence for the influence of sea ice. *Glob. Biogeochem. Cycle* **19**, 10.
- Gradinger, R. 2009. Sea-ice algae: Major contributors to primary production and algal biomass in the Chukchi and Beaufort Seas during May/June 2002. *Deep-Sea Research Part II-Topical Studies in Oceanography* **56**, 1201-1212.
- Harrison, W. G. and Cota, G. F. 1991. Primary production in polar waters -relation to nutrient availability. *Polar Research* **10**, 87-104.
- Heidam, N. Z. 1984. The components of the Arctic aerosol. *Atmospheric Environment (1967)* **18**, 329-343.
- Heide-Jorgensen, M. P., Laidre, K. L., Logsdon, M. L. and Nielsen, T. G. 2007. Springtime coupling between chlorophyll a, sea ice and sea surface temperature in Disko Bay, West Greenland. *Progress In Oceanography* **73**, 79-95.
- Heintzenberg, J. and Leck, C. 1994. SEASONAL-VARIATION OF THE ATMOSPHERIC AEROSOL NEAR THE TOP OF THE MARINE BOUNDARY-LAYER OVER SPITSBERGEN RELATED TO THE ARCTIC SULFUR CYCLE. *Tellus Ser. B-Chem. Phys. Meteorol.* **46**, 52-67.
- Heintzenberg, J. and Leck, C. 2012. The summer aerosol in the central Arctic 1991-2008: did it change or not? *Atmospheric Chemistry and Physics* **12**, 3969-3983.
- Holland, M. M., Bitz, C. M., Hunke, E. C., Lipscomb, W. H. and Schramm, J. L. 2006. Influence of the sea ice thickness distribution on polar climate in CCSM3. *J. Clim.* **19**, 2398-2414.
- Hop, H., Falk-Petersen, S., Svendsen, H., Kwasniewski, S., Pavlov, V. and co-authors 2006. Physical and biological characteristics of the pelagic system across Fram Strait to Kongsfjorden. *Progress In Oceanography* **71**, 182-231.
- Hunt, G. L. and Drinkwater, K. 2007. Introduction to the proceedings of the GLOBEC symposium on effects of climate variability on sub-Arctic marine ecosystems - Preface. *Deep-Sea Research Part II-Topical Studies in Oceanography* **54**, 2453-2455.
- Ito, A. and Kawamiya, M. 2010. Potential impact of ocean ecosystem changes due to global warming on marine organic carbon aerosols. *Glob. Biogeochem. Cycle* **24**.

- Jassby, A. D. and Powell, T. M. 1990. Detecting changes in ecological time-series. *Ecology* **71**, 2044-2052.
- Kahru, M., Brotas, V., Manzano-Sarabia, M. and Mitchell, B. G. 2011. Are phytoplankton blooms occurring earlier in the Arctic? *Global Change Biology* **17**, 1733-1739.
- Kerminen, V. M. and Leck, C. 2001. Sulfur chemistry over the central Arctic Ocean during the summer: Gas-to-particle transformation. *Journal of Geophysical Research-Atmospheres* **106**, 32087-32099.
- King, M. D., Menzel, W. P., Kaufman, Y. J., Tanré, D., Gao, B.-C. and co-authors 2003. Cloud and aerosol properties, precipitable water, and profiles of temperature and water vapor from MODIS. *Geoscience and Remote Sensing, IEEE Transactions on* **41**, 442-458.
- Kwok, R. and Rothrock, D. A. 2009. Decline in Arctic sea ice thickness from submarine and ICESat records: 1958-2008. *Geophys. Res. Lett.* **36**.
- Lana, A., Bell, T. G., Simo, R., Vallina, S. M., Ballabrera-Poy, J. and co-authors 2011. An updated climatology of surface dimethylsulfide concentrations and emission fluxes in the global ocean. *Glob. Biogeochem. Cycle* **25**.
- Leck, C., Bigg, E. K., Covert, D. S., Heintzenberg, J., Maenhaut, W. and co-authors 1996. Overview of the atmospheric research programme during the International Arctic Ocean Expedition of 1991 (IAOE-91) and its scientific results. *Tellus* **48B**, 136-155.
- Leck, C. and Bigg, E. K. 2005. Biogenic particles in the surface microlayer and overlaying atmosphere in the central Arctic Ocean during summer. *Tellus Ser. B-Chem. Phys. Meteorol.* **57**, 305-316.
- Leck, C. and Bigg, E. K. 2010. New Particle Formation of Marine Biological Origin. *Aerosol Science and Technology* **44**, 570-577.
- Lee, S. H., McRoy, C. P., Joo, H. M., Gradinger, R., Cui, X. H. and co-authors 2011. Holes in Progressively Thinning Arctic Sea Ice Lead to New Ice Algae Habitat. *Oceanography* **24**, 302-308.
- Leu, E., Soreide, J. E., Hessen, D. O., Falk-Petersen, S. and Berge, J. 2011. Consequences of changing sea-ice cover for primary and secondary producers in the European Arctic shelf seas: Timing, quantity, and quality. *Progress In Oceanography* **90**, 18-32.
- Levasseur, M. 2013. Impact of Arctic meltdown on the microbial cycling of sulphur. *Nature Geosci* **6**, 691-700.
- Longhurst, A. R. 2007. *Ecological Geography of the Sea*. San Diego, Academic Press.
- Loose, B., Miller, L. A., Elliott, S. and Papakyriakou, T. 2011. Sea Ice Biogeochemistry and Material Transport Across the Frozen Interface. *Oceanography* **24**, 202-218.
- Luce, M., Levasseur, M., Scarratt, M. G., Michaud, S., Royer, S. J. and co-authors 2011. Distribution and microbial metabolism of dimethylsulfoniopropionate and dimethylsulfide during the 2007 Arctic ice minimum. *J. Geophys. Res.-Oceans* **116**.
- Matrai, P. A., Tranvik, L., Leck, C. and Knulst, J. C. 2008. Are high Arctic surface microlayers a potential source of aerosol organic precursors? *Marine Chemistry* **108**, 109-122.

- Miller, A. J., M. A. Alexander, G. J. Boer, F. Chai, K. Denman and co-authors 2003. Potential Feedbacks Between Pacific Ocean Ecosystems and Interdecadal Climate Variations. *Bulletin American Meteorological Society* **84**, 617-633.
- Norman, A., Sanusi, A., Toom-Saunty, D., Gong, S. and Barrie, L. 2005. Arctic Biogenic Aerosol Sulphate Using Isotope Apportionment Techniques: 1993-2003. In: Proceedings of the AGU Fall Meeting Abstracts, 2005.
- Orellana, M. V., Matrai, P. A., Leck, C., Rauschenberg, C. D., Lee, A. M. and co-authors 2011. Marine microgels as a source of cloud condensation nuclei in the high Arctic. *Proc. Natl. Acad. Sci. U. S. A.* **108**, 13612-13617.
- Osthoff, H. D., Bates, T. S., Johnson, J. E., Kuster, W. C., Goldan, P. and co-authors 2009. Regional variation of the dimethyl sulfide oxidation mechanism in the summertime marine boundary layer in the Gulf of Maine. *Journal of Geophysical Research-Atmospheres* **114**.
- Pabi, S., van Dijken, G. L. and Arrigo, K. R. 2008. Primary production in the Arctic Ocean, 1998-2006. *J. Geophys. Res.-Oceans* **113**.
- Park, K.-T., Lee, K., Yoon, Y.-J., Lee, H.-W., Kim, H.-C. and co-authors 2013. Linking atmospheric dimethyl sulfide and the Arctic Ocean spring bloom. *Geophys. Res. Lett.* **40**, 155-160.
- Post, E., Bhatt, U. S., Bitz, C. M., Brodie, J. F., Fulton, T. L. and co-authors 2013. Ecological Consequences of Sea-Ice Decline. *Science* **341**, 519-524.
- Qu, B., Gabric, A. J., Zhu, J., Lin, D., Qian, F. and co-authors 2012. Correlation between sea surface temperature and wind speed in Greenland Sea and their relationship to NAO variability. *Water Science and Engineering* **5**, 304-315.
- Quinn, P. K., Shaw, G., Andrews, E., Dutton, E. G., Ruoho-Airola, T. and co-authors 2007. Arctic haze: current trends and knowledge gaps. *Tellus Ser. B-Chem. Phys. Meteorol.* **59**, 99-114.
- Remer, L. A., Tanré, D., Kaufman, Y. J., Ichoku, C., Mattoo, S. and co-authors 2002. Validation of MODIS aerosol retrieval over ocean. *Geophys. Res. Lett.* **29**, MOD3-1-MOD3-4.
- Remer, L. A., Kleidman, R. G., Levy, R. C., Kaufman, Y. J., Tanre, D. and co-authors 2008. Global aerosol climatology from the MODIS satellite sensors. *Journal of Geophysical Research-Atmospheres* **113**.
- Rempillo, O., Seguin, A. M., Norman, A. L., Scarratt, M., Michaud, S. and co-authors 2011. Dimethyl sulfide air-sea fluxes and biogenic sulfur as a source of new aerosols in the Arctic fall. *Journal of Geophysical Research-Atmospheres* **116**.
- Rey, F., Noji, T. T. and Miller, L. A. 2000. Seasonal phytoplankton development and new production in the central Greenland Sea. *Sarsia* **85**, 329-344.
- Richardson, K., Markager, S., Buch, E., Lassen, M. F. and Kristensen, A. S. 2005. Seasonal distribution of primary production, phytoplankton biomass and size distribution in the Greenland Sea. *Deep-Sea Research Part I-Oceanographic Research Papers* **52**, 979-999.
- Rudels, B., Larsson, A. M. and Sehlstedt, P. I. 1991. Stratification and water mass formation in the Arctic Ocean - some implications for the nutrient distribution. *Polar Research* **10**, 19-31.
- Russell, L. M., Hawkins, L. N., Frossard, A. A., Quinn, P. K. and Bates, T. S. 2010. Carbohydrate-like composition of submicron atmospheric particles and their

- production from ocean bubble bursting. *Proc. Natl. Acad. Sci. U. S. A.* **107**, 6652-6657.
- Schmitz, W. J. 1995. On the interbasin-scale thermohaline circulation. *Reviews of Geophysics* **33**, 151-173.
- Serreze, M. C., Barrett, A. P., Slater, A. G., Woodgate, R. A., Aagaard, K. and co-authors 2006. The large-scale freshwater cycle of the Arctic. *J. Geophys. Res.-Oceans* **111**.
- Sharma, S., Chan, E., Ishizawa, M., Toom-Sauntry, D., Gong, S. L. and co-authors 2012. Influence of transport and ocean ice extent on biogenic aerosol sulfur in the Arctic atmosphere. *Journal of Geophysical Research-Atmospheres* **117**.
- Spies, A., Brockmann, U. H. and Kattner, G. 1988. Nutrient regimes in the marginal ice-zone of the Greenland Sea in summer. *Marine Ecology-Progress Series* **47**, 195-204.
- Stroeve, J., Holland, M. M., Meier, W., Scambos, T. and Serreze, M. 2007. Arctic sea ice decline: Faster than forecast. *Geophys. Res. Lett.* **34**.
- Trevena, A. and Jones, G. 2012. DMS flux over the Antarctic sea ice zone. *Marine Chemistry* **134**, 47-58.
- Wang, M. H., Bailey, S. and McClain, C. R. 2000. SeaWiFS provided unique global aerosol optical property data. *Eos, American Geophysical Union* **81**, 197-202.
- Wang, M. Y. and Overland, J. E. 2009. A sea ice free summer Arctic within 30 years? *Geophys. Res. Lett.* **36**.
- Wassmann, P. 2011. Arctic marine ecosystems in an era of rapid climate change. *Progress In Oceanography* **90**, 1-17.
- Wassmann, P., Duarte, C. M., Agusti, S. and Sejr, M. K. 2011. Footprints of climate change in the Arctic marine ecosystem. *Global Change Biology* **17**, 1235-1249.
- Wassmann, P. and Reigstad, M. 2011. Future Arctic Ocean Seasonal Ice Zones and Implications for Pelagic-Benthic Coupling. *Oceanography* **24**, 220-231.
- Woodgate, R. A., Fahrbach, E. and Rohardt, G. 1999. Structure and transports of the East Greenland Current at 75 degrees N from moored current meters. *J. Geophys. Res.-Oceans* **104**, 18059-18072.
- Zar, J. H. 1999. *Biostatistical Analysis*. Upper Saddle River, N. J., Prentice-Hall.
- Zemmelink, H. J., Dacey, J. W. H., Houghton, L., Hintsa, E. J. and Liss, P. S. 2008. Dimethylsulfide emissions over the multi-year ice of the western Weddell Sea. *Geophys. Res. Lett.* **35**.
- Zhang, J. L., Spitz, Y. H., Steele, M., Ashjian, C., Campbell, R. and co-authors 2010. Modeling the impact of declining sea ice on the Arctic marine planktonic ecosystem. *Journal of Geophysical Research-Oceans*. **115**.

Table 1. Magnitude and Timing of Seasonal Peak in 8-day CHL by latitude sector

Year	CHL (mgm ⁻³)			Day of Year*		
	65-70°N	70-75°N	75-80°N	65-70°N	70-75°N	75-80°N
2003	1.6	2.1	1.5	113	145	169
2004	2.4	1.3	1.1	120	184	180
2005	0.9	1.8	1.5	145	177	177
2006	1.4	4.4	2.2	185	161	161
2007	1.2	3.6	1.2	145	153	161
2008	1.4	1.9	2.6	136	114	184
2009	1.5	1.2	1.7	129	121	201
2010	1.9	1.3	3.0	137	153	177
2011	1.8	2.4	3.9	129	153	153
2012	1.2	1.7	1.9	157	168	185
MEAN	1.5±0.4	2.2±1.0	2.1±0.9	140±20	153±22	175±14

*June 1 = Day 152

Table 2. Pearson's Correlation Coefficient (Significance*) for 8-day data

Year		CHL/AOD	CHL/ICE	AOD/ICE
2003	65-70°N	NS	–	–
	70-75°N	0.48 (p<0.04)	NS	NS
	75-80°N	NS	NS	NS
2004	65-70°N	0.40 (p<0.05)	–	–
	70-75°N	NS	NS	NS
	75-80°N	NS	NS	NS
2005	65-70°N	0.62 (p<0.01)	–	–
	70-75°N	NS	NS	NS
	75-80°N	NS	NS	NS
2006	65-70°N	NS	–	–
	70-75°N	NS	0.48 (p< 0.05)	NS
	75-80°N	NS	NS	0.53 (p<0.03)
2007	65-70°N	0.41 (p<0.07)	–	–
	70-75°N	NS	NS	NS
	75-80°N	NS	NS	0.62 (p<0.01)
2008	65-70°N	0.59 (p<0.01)	–	–
	70-75°N	NS	NS	NS
	75-80°N	NS	NS	NS
2009	65-70°N	NS	–	–
	70-75°N	NS	NS	NS
	75-80°N	NS	NS	0.57 (p<0.01)
2010	65-70°N	NS	–	–
	70-75°N	NS	NS	NS
	75-80°N	NS	NS	NS
2011	65-70°N	0.47 (p<0.04)	–	–
	70-75°N	NS	NS	NS
	75-80°N	NS	NS	0.53 (p<0.03)
2012	65-70°N	NS	–	–
	70-75°N	NS	NS	NS
	75-80°N	NS	NS	NS

*NS = Not statistically significant

FIGURE CAPTIONS

Figure 1 Site of study region in Greenland Sea (highlighted box is for 10°W-10°E, 65-80°N). The underlying map was obtained from NOAA (www.ngdc.noaa.gov/mgg/bathymetry/arctic/currentmap.html).

Figure 2 (a) Monthly CHL (mg m^{-3}) climatology (2003-12), in the three latitudinal sectors, and (b) standard deviations (mg m^{-3})

Figure 3 Hovmoller plots of climatological monthly mean (a) CHL (mg m^{-3}), (b) AOD and (c) ICE (%) in the study region, by latitude

Figure 4 CHL, AOD and ICE 8-day time series for 2003-2012 for (a) 65-70°N sector which was always ice-free, (b) 70-75°N where ice cover was <5% (omitted for clarity), (c) 75-80°N.

Figure 5 (a) Monthly AOD climatology (2003-2012), in the three latitudinal sectors, and (b) standard deviations, and (c) monthly AOD time series showing a summer secondary in some years

Figure 6 CHL and AOD 8-day time series in 65-70°N for (a) 2005 and (b) 2008.

Figure 7. DMS seawater concentrations in the study region, from the NOAA DMS climatology (1990-2008)

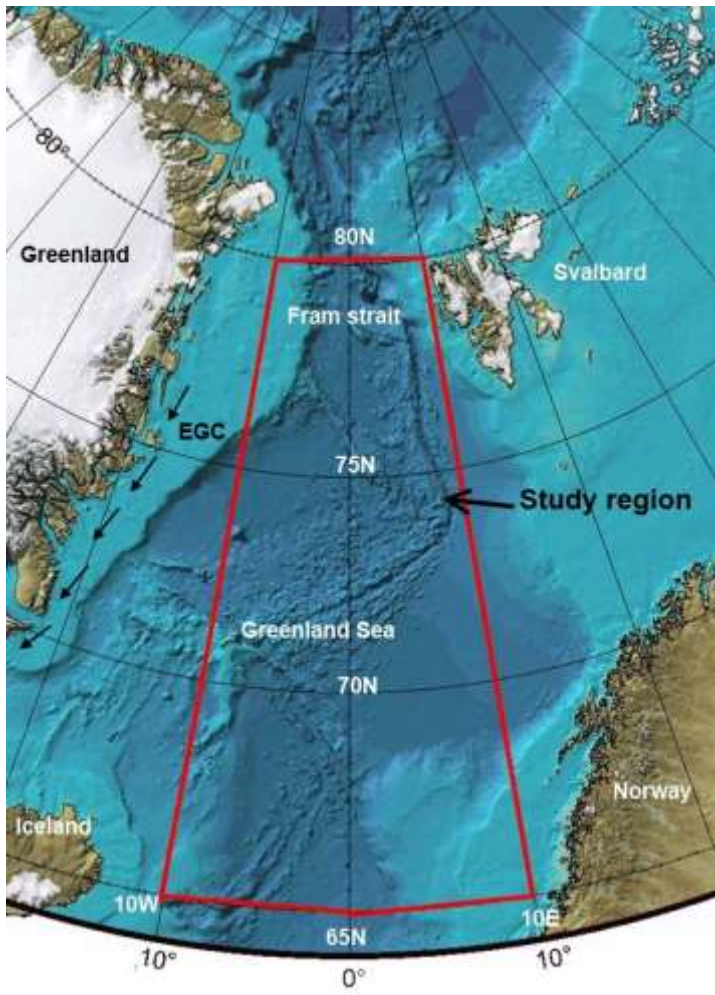


Figure 1: Map of the study region in the Greenland Sea

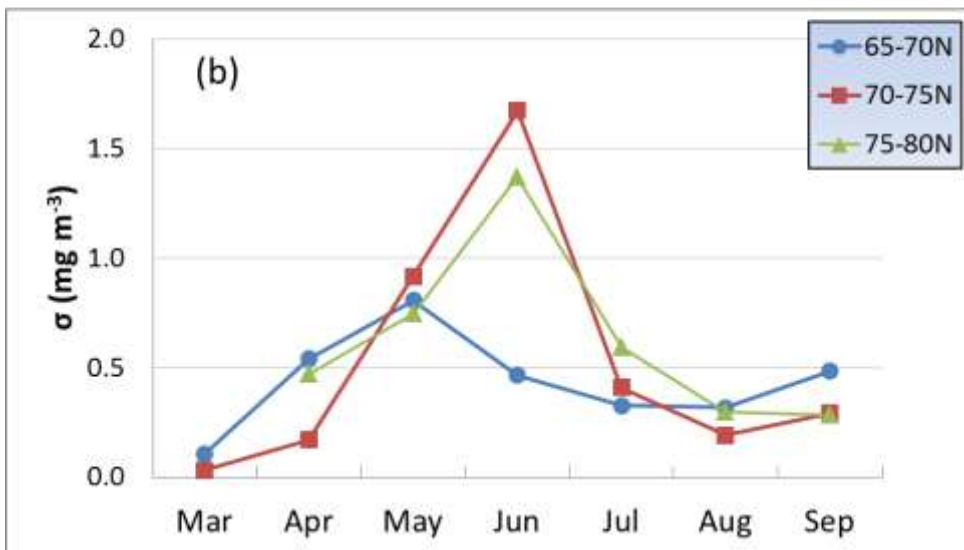
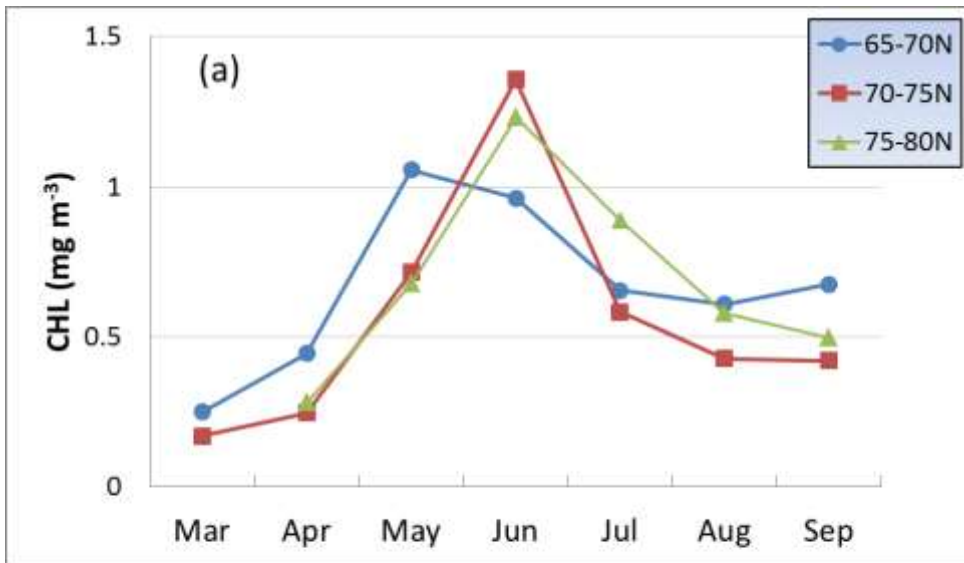
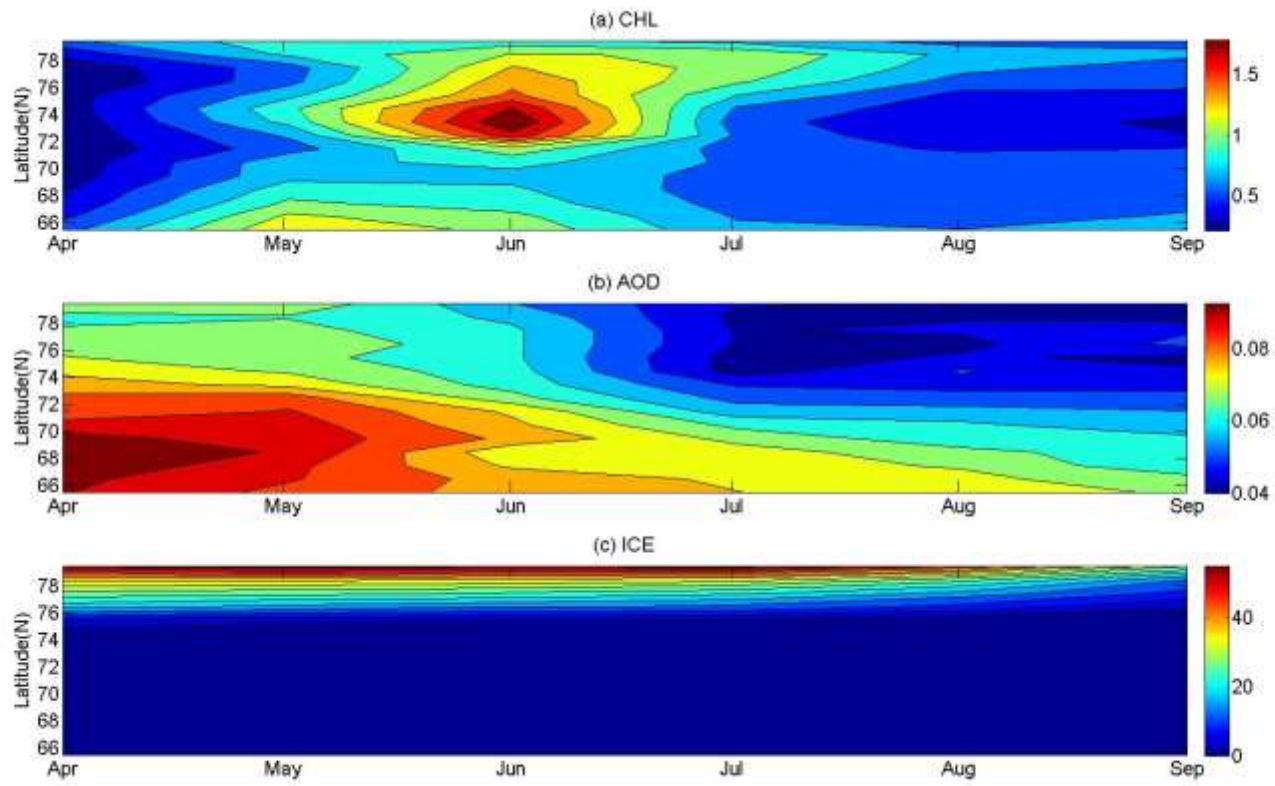


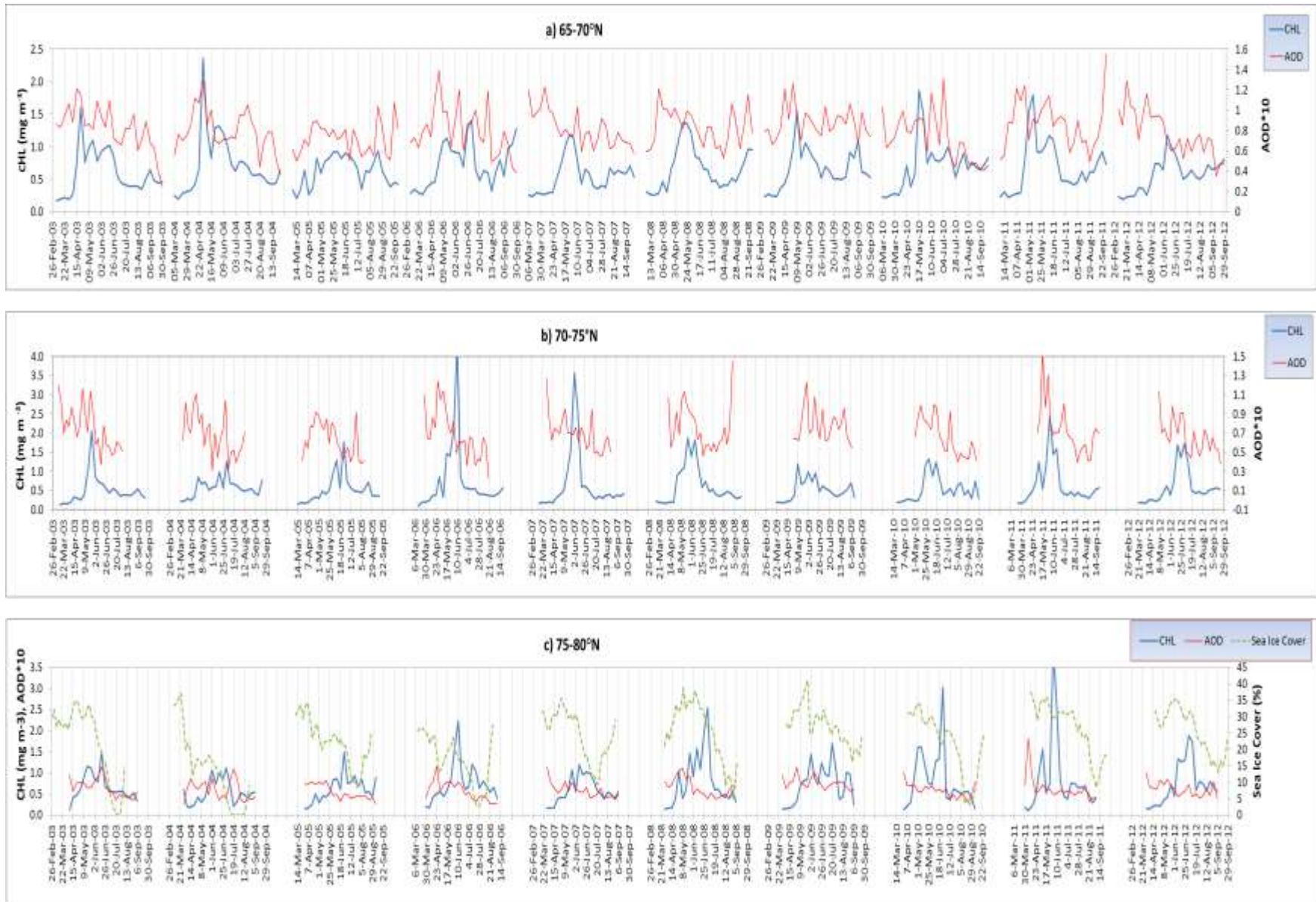
Figure 2.



1

2

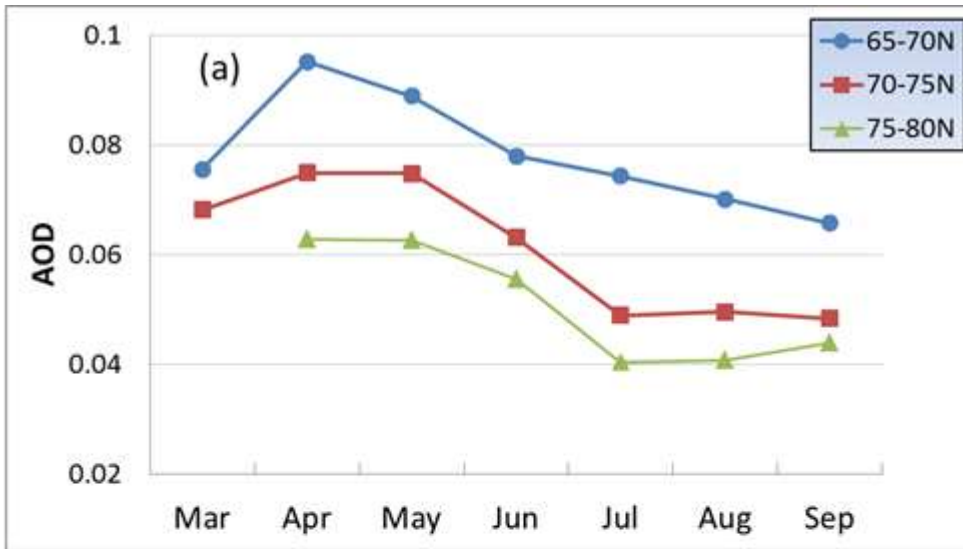
3 Figure 3.



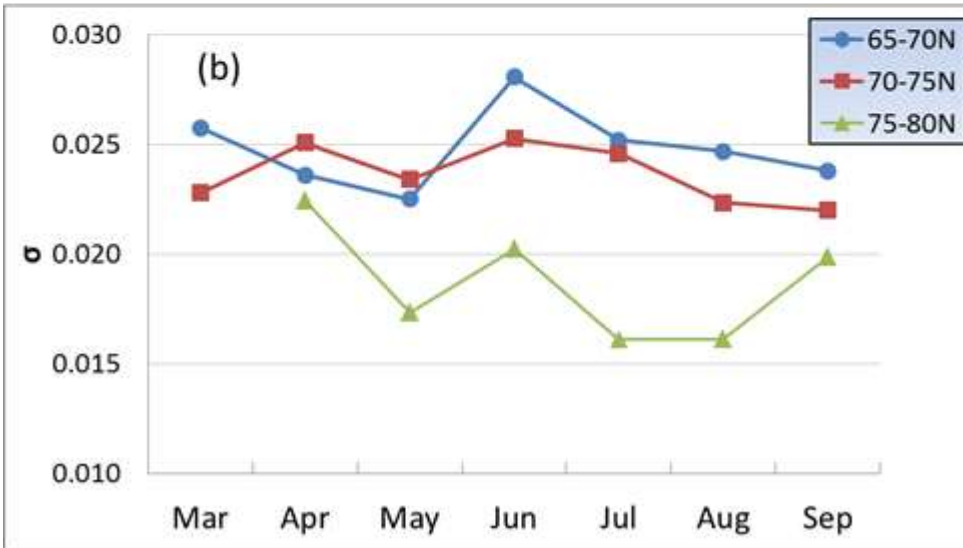
5 Figure 4.

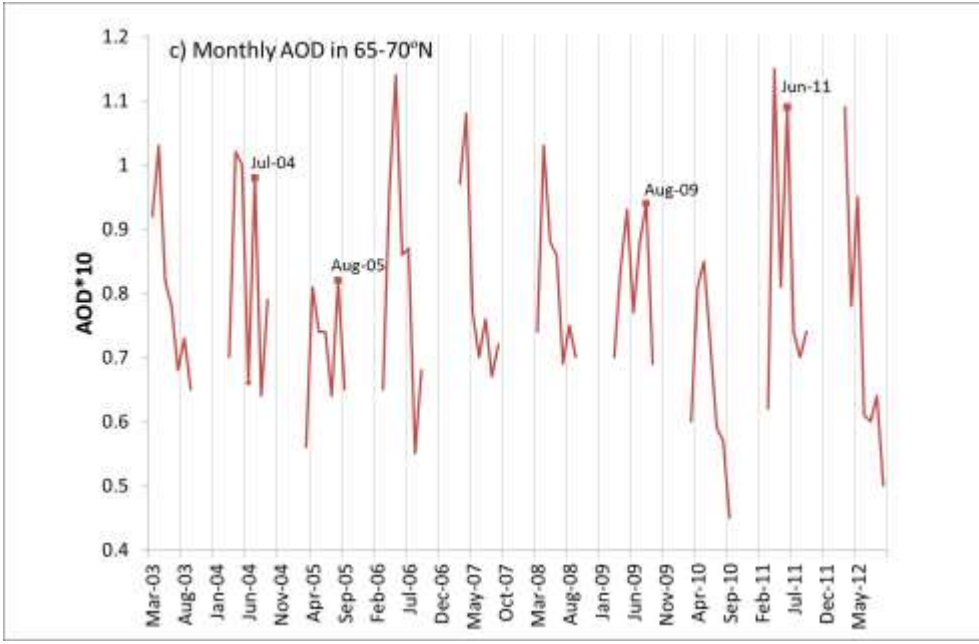
6

7



8



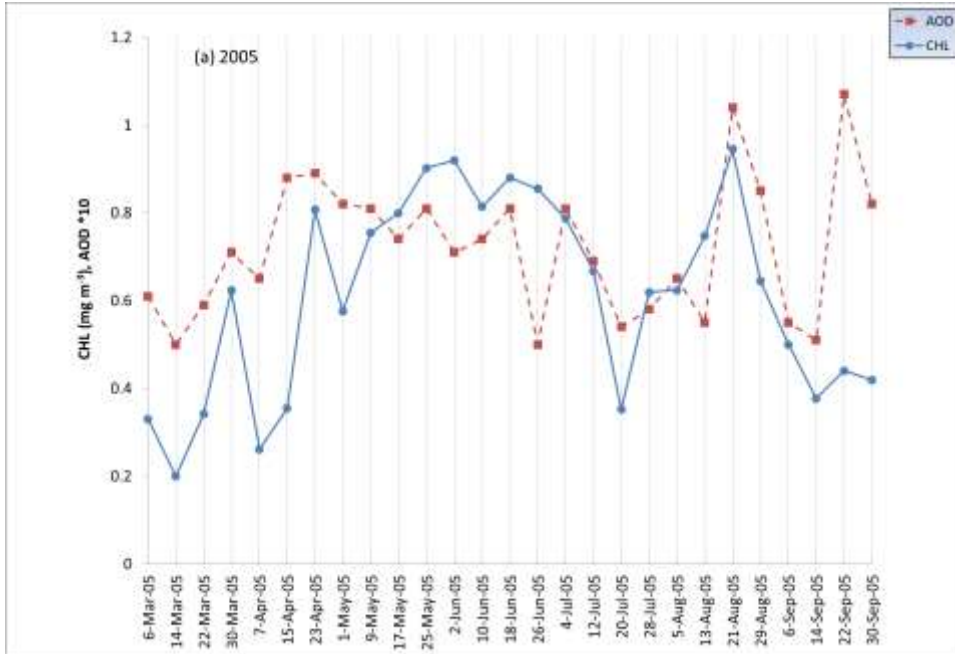


9

10 Figure 5.

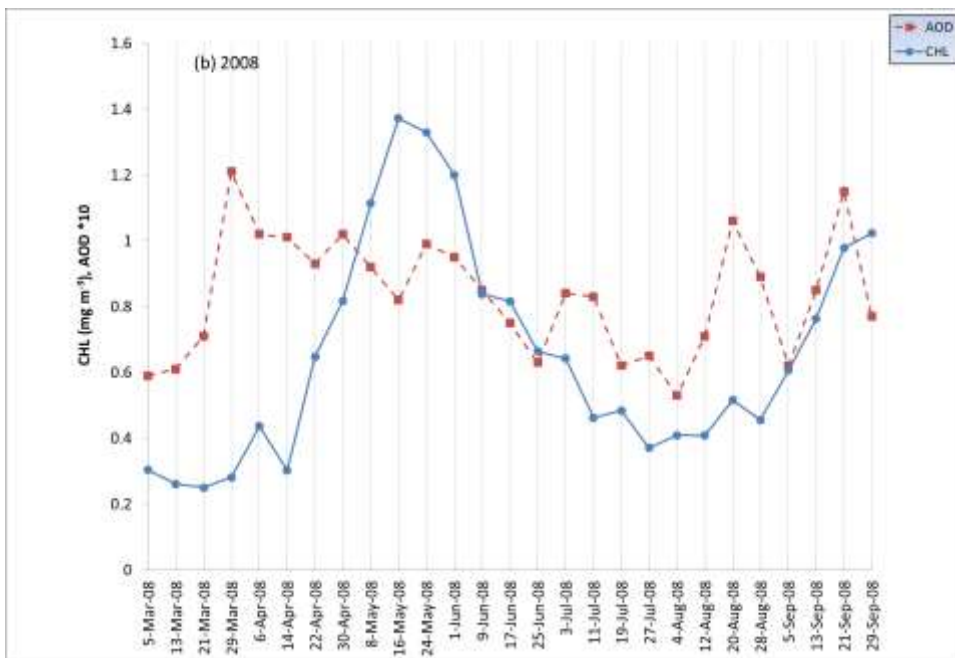
11

12



13

14

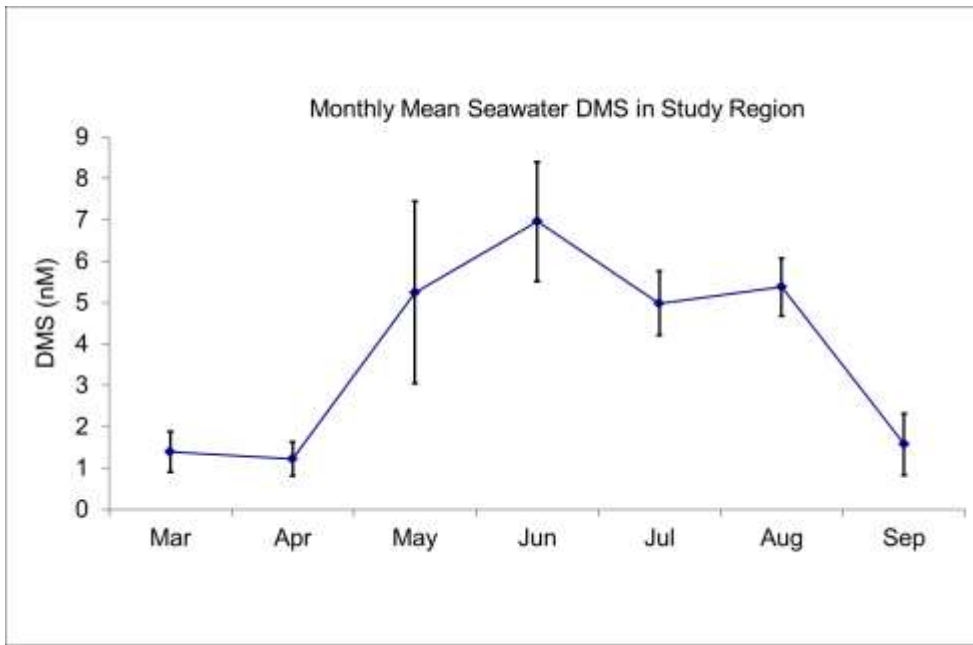


15

16

17 Figure 6.

18



19

20 Figure 7.